

SCIENTIFIC REPORTS



OPEN

Mast cells play role in wound healing through the ZnT2/GPR39/IL-6 axis

Keigo Nishida^{1,2}, Aiko Hasegawa^{2,7}, Satoru Yamasaki^{2,3}, Ryota Uchida¹, Wakana Ohashi^{2,8}, Yosuke Kurashima^{9,10,11,12,13,14,15}, Jun Kunisawa^{15,16}, Shunsuke Kimura^{17,19}, Toshihiko Iwanaga¹⁷, Hiroshi Watarai¹⁸, Koji Hase^{19,20}, Hideki Ogura²¹, Manabu Nakayama²², Jun-ichi Kashiwakura²³, Yoshimichi Okayama²⁴, Masato Kubo^{4,25}, Osamu Ohara⁵, Hiroshi Kiyono^{10,12,13,14,16}, Haruhiko Koseki⁶, Masaaki Murakami²⁶ & Toshio Hirano²⁷

¹Laboratory of Immune Regulation, Graduate School of Pharmaceutical Sciences, Suzuka University of Medical Science, 3500-3 Minamitamagaki-cho, Suzuka, Mie, 513-8670, Japan. ²Laboratory for Homeostatic Network, RIKEN Center for Integrative Medical Sciences (IMS), 1-7-22 Suehiro-cho, Tsurumi, Yokohama, Kanagawa, 230-0045, Japan. ³Laboratory for Immunotherapy, RIKEN Center for Integrative Medical Sciences (IMS), 1-7-22 Suehiro-cho, Tsurumi, Yokohama, Kanagawa, 230-0045, Japan. ⁴Laboratory for Cytokine Regulation, RIKEN Center for Integrative Medical Sciences (IMS), 1-7-22 Suehiro-cho, Tsurumi, Yokohama, Kanagawa, 230-0045, Japan. ⁵Laboratory for Integrative Genomics, RIKEN Center for Integrative Medical Sciences (IMS), 1-7-22 Suehiro-cho, Tsurumi, Yokohama, Kanagawa, 230-0045, Japan. ⁶Laboratory for Developmental Genetics, RIKEN Center for Integrative Medical Sciences (IMS), 1-7-22 Suehiro-cho, Tsurumi, Yokohama, Kanagawa, 230-0045, Japan. ⁷Department of Pediatrics, Shinshu University School of Medicine, 3-1-1 Asahi, Matsumoto, Nagano, 390-8621, Japan. ⁸Department of Molecular and Medical Pharmacology, Graduate School of Medicine and Pharmaceutical Sciences for Research, University of Toyama, Toyama, 930-0194, Japan. ⁹Department of Innovative Medicine, Graduate School of Medicine, Chiba University, 1-8-1 Inohana, Chuo-ku, Chiba, 260-8670, Japan. ¹⁰Division of Mucosal Immunology, IMSUT Distinguished Professor Unit, the Institute of Medical Science, The University of Tokyo, 4-6-1 Shirokanedai, Minato-ku, Tokyo, Japan. ¹¹Department of Mucosal Immunology, Graduate School of Medicine, Chiba University, 1-8-1 Inohana, Chuo-ku, Chiba, 260-8670, Japan. ¹²Division of Clinical Vaccinology, International Research and Development Center for Mucosal Vaccine, The Institute of Medical Science, The University of Tokyo, 4-6-1 Shirokanedai, Minato-ku, Tokyo, Japan. ¹³Institute for Global Prominent Research, Chiba University, 1-8-1 Inohana, Chuo-ku, Chiba, 260-8670, Japan. ¹⁴Chiba University-UC San Diego Center for Mucosal Immunology, Allergy and Vaccines (CU-UCSD cMAV), University of California San Diego, 9500 Gilman Dr. MC 0063, San Diego, CA, 92093-0063, United States. ¹⁵Laboratory of Vaccine Materials, Center for Vaccine and Adjuvant Research, and Laboratory of Gut Environmental System, National Institutes of Biomedical Innovation, Health and Nutrition (NIBIOHN), 7-6-8 Asagi Saito, Ibaraki, Osaka, 567-0085, Japan. ¹⁶Division of Mucosal Vaccines, International Research and Development Center for Mucosal Vaccines, The Institute of Medical Science, The University of Tokyo, 4-6-1 Shirokanedai, Minato-ku, Tokyo, 108-8639, Japan. ¹⁷Laboratory of Histology and Cytology, Department of Anatomy, Hokkaido University Graduate School of Medicine, Sapporo, 060-8638, Japan. ¹⁸Department of Immunology and Stem Cell Biology, Faculty of Medicine, Institute of Medical, Pharmaceutical and Health Sciences, Kanazawa University, 13-1 Takaramachi, Kanazawa, Ishikawa, 920-8640, Japan. ¹⁹Division of Biochemistry, Faculty of Pharmacy, Keio University, Tokyo, 105-8512, Japan. ²⁰International Research and Development Center for Mucosal Vaccine, The Institute of Medical Science, The University of Tokyo (IMSUT), 108-8639, Tokyo, Japan. ²¹Department of Microbiology, Hyogo College of Medicine 1-1, Mukogawa-cho, Nishinomiya, 663-8501, Japan. ²²Laboratory of Medical Omics Research, Department of Frontier Research and Development, Kazusa DNA Research Institute, 2-6-7 Kazusa-Kamatari, Kisarazu, Chiba, 292-0818, Japan. ²³Laboratory of Immunology, Graduate School of Pharmaceutical Sciences, Hokkaido University, Sapporo, 060-0812, Japan. ²⁴Allergy and Immunology Project Team, Center for Allergy, Center for Medical Education, Nihon University School of Medicine, 30-1 Oyaguchi Kamicho Itabashi-Ku, Tokyo, 173-8610, Japan. ²⁵Division of Molecular Pathology, Research Institute for Biomedical Science, Tokyo University of Science, 2669 Yamazaki, Noda-shi, Chiba, 278-0022, Japan. ²⁶Division of Molecular Psychoimmunology, Institute for Genetic Medicine and Graduate School of Medicine, Hokkaido University, Sapporo, 060-815, Japan. ²⁷Headquarters, National Institutes for Quantum and Radiological Science and Technology, 4-9-1 Anagawa, Inage-ku, Chiba, 263-8555, Japan. Correspondence and requests for materials should be addressed to K.N. (email: knishida@suzuka-u.ac.jp)

Received: 11 July 2018
Accepted: 11 July 2019
Published online: 25 July 2019

Zinc (Zn) is an essential nutrient and its deficiency causes immunodeficiency and skin disorders. Various cells including mast cells release Zn-containing granules when activated; however, the biological role of the released Zn is currently unclear. Here we report our findings that Zn transporter ZnT2 is required for the release of Zn from mast cells. In addition, we found that Zn and mast cells induce IL-6 production from inflammatory cells such as skin fibroblasts and promote wound healing, a process that involves inflammation. Zn induces the production of a variety of pro-inflammatory cytokines including IL-6 through signaling pathways mediated by the Zn receptor GPR39. Consistent with these findings, wound healing was impaired in mice lacking IL-6 or GPR39. Thus, our results show that Zn and mast cells play a critical role in wound healing through activation of the GPR39/IL-6 signaling axis.

Zinc (Zn) is an essential nutrient, and its deficiency causes growth retardation, immunodeficiency, and skin disorders^{1–4}. Zn is critically involved in various physiological functions including development, immunity and wound healing^{5–9}, and impaired wound healing can be reversed by Zn supplementation^{10,11}. Indeed, many metalloenzymes and transcription factors require Zn to execute their functions¹². Zn also acts as an intracellular signaling molecule, and changes in its intracellular concentration in response to extracellular stimuli affect a variety of signaling pathways^{13–19}. It has been reported that Zn also functions as a neurotransmitter^{20,21}. Zn released from activated neurons appears to regulate the overall excitability of the brain through its effects on glutamate and γ -aminobutyric acid (GABA) receptors, and it is also considered important for synaptic plasticity^{22,23}. It has also been reported that mast cell granules are rich in Zn and they release Zn like neurotransmitter^{24–26}. These reports suggest that Zn in mast cell granules may be involved in mast cell-dependent inflammatory or allergic responses. However, it is currently unclear how Zn released from mast cell regulates inflammatory responses such as those involved in wound repair.

Recent studies have shown that Zn is an endogenous agonist for GPR39, an orphan receptor that is structurally and functionally related to G-protein-coupled receptors²⁷. GPR39 is ubiquitously expressed in peripheral tissues including the skin, gut and brain^{28–30}. In addition, accumulating *in vitro* evidence suggests that GPR39 mediates Zn-dependent signaling in keratinocytes, colonocytes and neurons³¹. Therefore, GPR39 may function as a physiological receptor for Zn released from several different types of cells.

To determine whether Zn released from mast cells plays an important role in inflammatory processes such as those involved in wound healing, and to explore the mechanism by which Zn functions in these processes, we used genetically engineered mice that have mast cells defective in localizing Zn to granules. The homeostasis of cellular Zn is regulated by two major families of mammalian Zn transporters: the Zip family that increases intracellular Zn, and the ZnT family that extrudes Zn from the cytoplasm either directly into the extracellular environment or into intracellular secretory vesicles. The ZnT family has nine known members^{32–36}. The accumulation of Zn in cellular organelles such as granules depends on the members of the ZnT family³⁷. For example, ZnT3 is essential for the accumulation of Zn in synaptic vesicles of the neuron³⁸. Therefore, we set out to identify the ZnT family member most closely associated with mast cell granules, and examined its effect on Zn accumulation in these granules by generating mutant mice containing a deletion in the relevant ZnT family member.

In this study, we identified ZnT2 as the ZnT family member responsible for Zn accumulation in mast cell granules by using *ZnT2*^{-/-} mice. We also showed that Zn and mast cells play a role in wound healing by inducing IL-6 production via activation of GPR39 at inflammatory sites of several types of cells. Furthermore, we obtained genetic evidence that both IL-6 and GPR39 are required for cutaneous wound healing. Collectively, our findings indicate that Zn is a pro-inflammatory signal and that the Zn/GPR39/IL-6 axis plays a critical role in wound healing.

Results

ZnT2 is required for the release of Zn from mast cells. To investigate the role of Zn in mast cell granules, we first sought to identify the Zn transporter(s) that transport Zn into this organelle. We examined the expression level of each ZnT family member in bone marrow-derived mast cells (BMMCs) by querying the Reference Database of Immune Cells (ReFDIC)³⁹, and found that *ZnT2* is among the highly expressed *ZnT*s in BMMCs (Supplemental Fig. 1). Next, we examined the subcellular localization of ZnT2 in BMMCs by confocal microscopy, and detected the transporter in the cytoplasm, colocalized with a granule marker CD63 (Fig. 1A and Supplemental Fig. 2). To confirm this result, we performed the electron microscopic observation of mast cells with anti-CD63 (granule marker) and anti-ZnT2 antibodies. As shown in Fig. 1B, CD63 and ZnT2 signals were detected around the granule membrane of mast cells. When the BMMC-derived organelles were fractionated by sucrose gradient centrifugation, ZnT2 was mainly detected in CD63-enriched fractions (Fig. 1C and Supplemental Fig. 3). These results identified ZnT2 as a candidate molecule responsible for transporting Zn into mast cell granules.

To clarify the function of ZnT2, we used *ZnT2*^{-/-} mice⁴⁰. BMMCs derived from *ZnT2*^{+/-}, but not *ZnT2*^{-/-} bone marrow, expressed ZnT2 protein, confirming gene inactivation in the mutant (Supplemental Figs 4 and 5). No difference was found in mast cell development between the two genotypes *in vivo* or *in vitro*. As shown in Supplemental Fig. 6A–C, there was no significant difference between the two morphotypes in the morphology of skin mast cells, the ratio of peritoneal mast cells as well as the expression of c-kit and Fc ϵ RI on the surface of cultured mast cells. We next investigated the Zn content in BMMC-derived mast cell granules from *ZnT2*^{-/-} and WT mice by confocal microscopy using a Zn probe FluoZin-3. FluoZin-3 signal was clearly detected in granule-like structures in the cytoplasm of control BMMCs but not in *ZnT2*^{-/-} BMMCs (Fig. 1D). Consistent with this observation, the intensity of FluoZin-3 signal was also significantly reduced in the *ZnT2*^{-/-} mast cells as detected by flow cytometry (Fig. 1E). As these findings indicated that ZnT2 is important for the accumulation

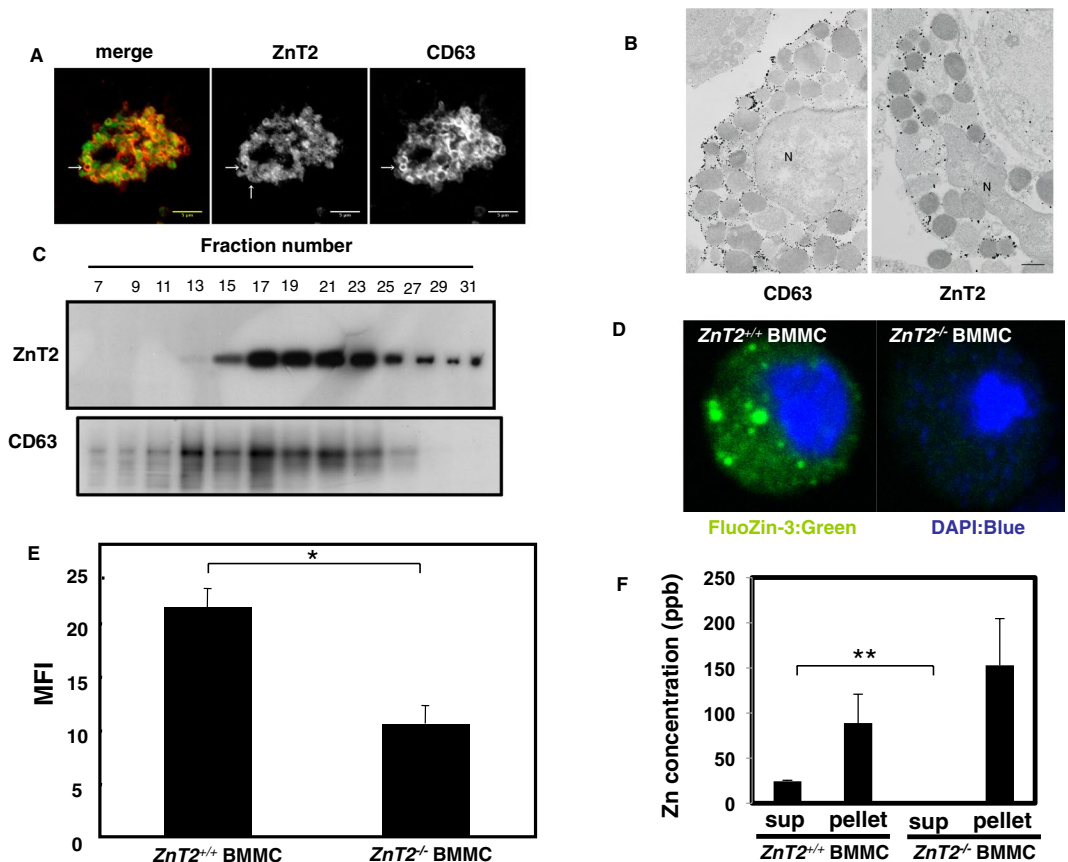


Figure 1. ZnT2 is required for Zn release from stimulated mast cells. (A) Double immunostaining of CD63 (red) and ZnT2 (green) in mast cells. ZnT2 is clearly localized at the periphery of granules indicated by an arrow. Scale bars: 5 μ m (B) Gold particles showing the immunoreactivities for CD63 and ZnT2 are distributed mainly along the membrane of granules. N: nucleus, scale bar: 1 μ m (C) Nuclear-free cell extract from BMMCs was fractionated by centrifugation in a 0.4–2.0 M sucrose gradient. Proteins in each fraction were analyzed by immunoblotting using anti-ZnT2 and -CD63 antibodies. (D) Confocal microscopy of intracellular granule-resident Zn using the Zn indicator FluoZin-3 (green) in BMMCs. Nuclei were stained with DAPI (blue). (E) FACS analysis of intracellular granule-resident Zn using FluoZin-3 in BMMCs. The mean fluorescence intensity (MFI) is shown. Values represent the mean \pm SD. * P < 0.05 (two-tailed Student's t-test). (F) *ZnT2*^{+/+} and *ZnT2*^{-/-} BMMCs were stimulated with 1 μ M ionomycin for 30 min. Zn released into the culture supernatant was quantified by ICP-AES. Values represent the mean \pm SD. ** P < 0.01 (two-tailed Student's t-test). A representative dataset from two (for c, f) or three (for e) experiments, each of which gave similar results, is shown.

of Zn in mast cell granules, we investigated whether Zn can be released from *ZnT2*^{-/-} BMMCs by inductively coupled plasma-atomic emission spectroscopy (ICP-AES) analysis, and found that Zn was not released following ionomycin stimulation (Fig. 1F). To determine whether this defect altered mast cell function, we examined the ability of *ZnT2*^{-/-} BMMCs to degranulate, synthesize and produce cytokines. *ZnT2*^{-/-} BMMCs released similar amounts of β -hexosaminidase to WT BMMCs and produced comparable amounts of IL-6 and TNF α in response to Fc ϵ RI or LPS stimulation (Supplemental Fig. 7A–C), indicating that ZnT2 has little influence on the secretion mechanisms involved in the release of β -hexosaminidase, IL-6 or TNF α in BMMCs.

Mast cell ZnT2 is required for normal wound healing. Given the defective Zn release from *ZnT2*^{-/-} BMMCs, we next examined the role of Zn localized in intracellular granules in a mast cell-mediated inflammatory process using mutant mice. Wound healing is a highly ordered and well-coordinated process involving inflammation, cell proliferation, matrix deposition and tissue remodeling⁴¹. We and others have shown that mast cells are involved in this process using mast cell-deficient mice such as *Kit*^{W-sh/W-sh} mice and MasTRECK mice (Supplemental Fig. 8A,B). To evaluate the role of ZnT2 in mast cell granules in wound healing, *ZnT2*^{-/-} and control mice were subjected to full-thickness excision of shaved dorsal skin and wounds were monitored for up to 12 days. In control mice, the wound area was reduced to 30% of the original area 7 days after injury. However, *ZnT2*^{-/-} mice exhibited impaired wound closure, and the wound remained at 60% of the original area 7 days after injury (Fig. 2A).

To determine whether defective wound healing in *ZnT2*^{-/-} mice was caused by ZnT2 deficiency in mast cells and not by factors derived from other cells or tissues in the wound environment, we engrafted mast cells from control or *ZnT2*^{-/-} mice into *Kit*^{W-sh/W-sh} mice, in which mast cells are not observed. The number of mast cells per mm² in the

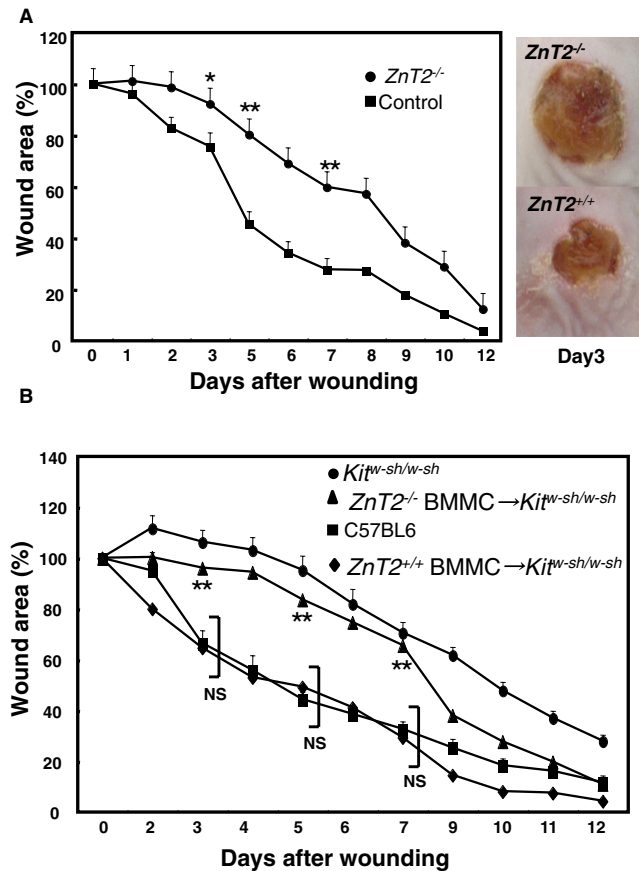


Figure 2. ZnT2 is important for normal wound healing. **(A)** Wound repair in *ZnT2*^{-/-} and control mice. Changes in the wound area over time were expressed as a percentage of the original wound area. Values represent the mean + SEM. Filled circles, *ZnT2*^{-/-} (n = 11 animals; female = 7, male = 4); filled squares, control (n = 12; female = 7, male = 5). *P < 0.05, **P < 0.01 (two-tailed Student's t-test), *ZnT2*^{-/-} compared with control mice. Photographs show the macroscopic changes in skin wounds 3 days after wounding in *ZnT2*^{-/-} and control mice. **(B)** Wound closure in *Kit*^{W-sh/Kit}^{W-sh} mice (n = 5 animals; female = 2, male = 3) whose dermis was previously reconstituted with control (n = 16 animals; female = 8, male = 8) or *ZnT2*^{-/-} (n = 13; female = 6, male = 7) BMMCs. Data were pooled from at least 3 independent experiments. Values represent the mean + SEM; **P < 0.01 comparing C57BL/6 and *ZnT2*^{-/-} mast cell-reconstituted *Kit*^{W-sh/Kit}^{W-sh} mice (*ZnT2*^{-/-} BMMCs → *Kit*^{W-sh/Kit}^{W-sh} mice); NS P > 0.05 comparing C57BL/6 and *ZnT2*^{+/+} mast cell-reconstituted *Kit*^{W-sh/Kit}^{W-sh} mice (*ZnT2*^{+/+} BMMCs → *Kit*^{W-sh/Kit}^{W-sh} mice).

dermis from the back skin in both groups of mice was comparable (Supplemental Fig. 9). The engraftment of BMMCs from control mice, but not *ZnT2*^{-/-} mice, restored wound healing in the *Kit*^{W-sh/Kit}^{W-sh} mice (Fig. 2B). Collectively, these findings demonstrate that the expression of ZnT2 in mast cells is required in the early stage of normal wound healing, although we do not completely exclude the possible involvement of ZnT2 expressed by other cells or tissues.

ZnT2 regulates IL-6 production during wound healing. Wound healing is characterized by three sequential phases: inflammation, proliferation and remodeling⁴². These phases are regulated by various cytokines, including IL-6 and TGF-β. It has been suggested that mast cells are involved in all three phases⁴³. We first examined whether ZnT2 was involved in the inflammation phase by making an aseptic, full-thickness incision on the back of control and *ZnT2*^{-/-} mice, as previously described⁴⁴. The expression of *Il-6* and *Tgf-β1* mRNA was higher at the wound edge than in the intact skin of unwounded control mice (Fig. 3A). However, the mRNA expression of *Il-6*, but not *Tgf-β1*, was significantly reduced in the wounded *ZnT2*^{-/-} mice compared to wounded controls (Fig. 3A). This result suggested that *il6* mRNA expression after skin injury is regulated by Zn released via ZnT2. To confirm that IL-6 is required for wound healing, we performed the wound-healing assay on *Il-6*^{-/-} mice. Wound closure was impaired in the absence of IL-6 in mice 2 to 11 days after injury. The wound area was 70% of the original 7 days after injury, and was consistently larger in the *Il-6*^{-/-} than the control mice from 2 to 11 days after injury (Fig. 3B). These observations raised the possibility that Zn derived from mast cells induced inflammatory cytokines such as IL-6 to promote cutaneous wound healing.

Zn can induce *Il-6* gene expression through a Zn receptor GPR39. To test whether Zn can induce the expression of cytokines in immune cells, we measured cytokine gene induction in Raw264.7 macrophage cell lines, mouse embryonic fibroblasts (MEFs), bone marrow-derived dendritic cells (BMDCs), and mouse macrophage treated with 50 μM Zn. We chose this Zn concentration for our experiments based on the previous

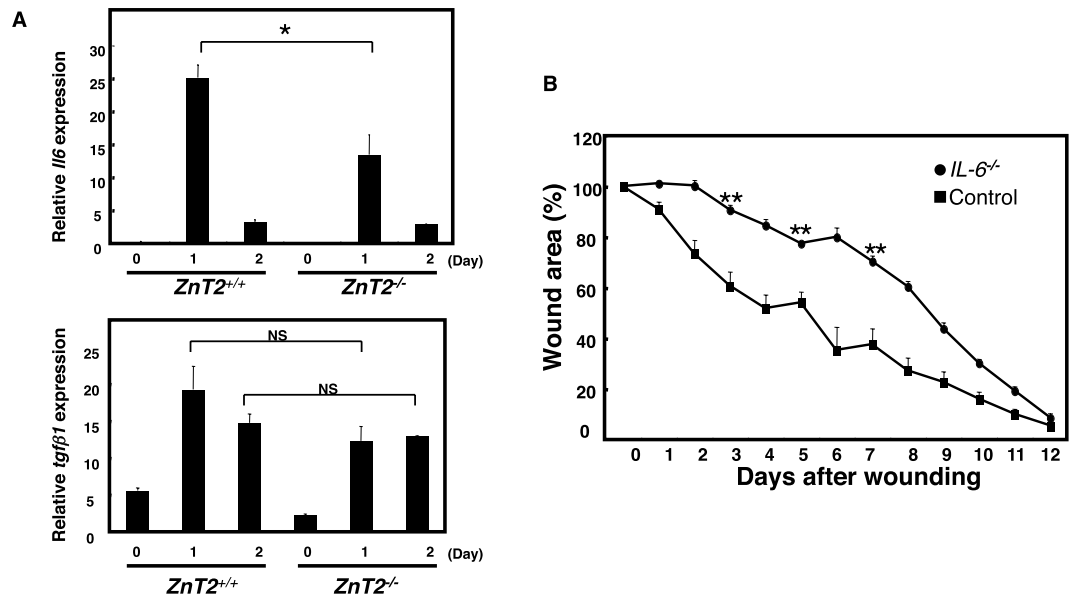


Figure 3. *ZnT2* is involved in *Il-6* gene induction during wound healing. (A) *Il-6* and *Tgf-β1* mRNA expression in 6 mm of skin surrounding the wound edge 0, 1, and 2 days after injury, quantified by real-time PCR. (B) Wound repair was evaluated in *Il-6*^{-/-} and control mice. Values represent the mean + SEM. Filled circles, *Il-6*^{-/-} (n = 9 animals; female = 5, male = 4); filled squares, control. (n = 9 animals; female = 5, male = 4). **P < 0.01 (two-tailed Student's t-test), *Il-6*^{-/-} compared with control mice.

report²⁸. Zn induced not only *Il-6* mRNA but also mRNAs for other inflammatory cytokines in all cell types tested (Fig. 4A–D). Consistent with increased mRNA expression, the levels of IL-6, TNF α , RANTES, and G-CSF protein were elevated in Zn-treated Raw264.7 cells (Fig. 4E).

Extracellular Zn has been reported to be a ligand of the GPR39 receptor^{45,46}. We therefore examined the role of GPR39 in Zn-dependent cytokine gene expression by gene silencing using siRNA constructs. Zn-triggered cytokine gene induction in MEFs was markedly reduced after GPR39 silencing (Fig. 4F), indicating that the response was mediated by GPR39.

Zn can regulate the PKC/MAPK/C/EBP signaling cascade. We next treated Raw264.7 cells with signaling pathway inhibitors in the presence or absence of Zn. Among the various inhibitors tested, the protein kinase C (PKC) inhibitor Gö6976 and the G-protein inhibitor GDP β S significantly blocked the effect of Zn on cytokine gene expression (Fig. 5A), while the response was not blocked by the protein kinase A (PKA) inhibitor 14–22, the PI-3K inhibitor wortmannin, or the calcineurin inhibitor cyclosporin A (CsA) (Fig. 5A). Based on these results, we tested whether Zn regulates PKC phosphorylation and found that it did (Fig. 5B and Supplemental Fig. 10). siRNA targeting PKC α abolished Zn-mediated *Il-6* gene induction in MEFs, confirming the involvement of PKC in Zn-mediated cytokine gene induction (Fig. 5C). PKC activation is known to induce the phosphorylation of ERK, and we found that Zn induced ERK phosphorylation, confirming that ERK acts downstream of PKC in this pathway (Fig. 5D and Supplemental Fig. 11). Consistent with this finding, the MAPK inhibitor U0126 significantly reduced Zn-mediated cytokine gene induction (Fig. 5E).

We next examined the molecular mechanism of *Il-6* gene regulation. Analysis of *Il-6* promoter revealed putative binding sites for several transcription factors including AP1, CRE, and C/EBP (Supplemental Fig. 12). To dissect the transcription factor(s) involved in Zn-mediated cytokine gene induction, we performed a luciferase reporter assay using the *Il-6* promoter and constructs containing mutated transcription factor binding sites (Supplemental Fig. 12). Zn-mediated luciferase activity was decreased in the C/EBP mutant (Fig. 5F), suggesting that C/EBP is involved in Zn-mediated cytokine gene induction. *Il-6* gene induction was also suppressed in cells transfected with *Cebpb* siRNA (Fig. 5G), confirming the involvement of C/EBP. Taken together, these data are consistent with the mechanism by which Zn activates the GPR39/PKC/ERK/C/EBP signaling pathway and induces cytokine gene expression (Fig. 5H).

GPR39 is required for normal wound healing. To examine the role of GPR39 in wound healing, we first confirmed that *Gpr39* was expressed in the hypodermis under the injury site (Fig. 6A). The *gpr39* signal was not detected in unwounded skin in our *in situ* hybridization experiment (Supplemental Fig. 13). Double *in situ* analysis indicated that *Gpr39* was expressed in fibroblasts (Fig. 6B). Next, we investigated whether *gpr39*-expressed fibroblasts can produce IL-6 upon wound stimulation. We sorted skin fibroblasts from unwounded or wounded skin and checked the expression of IL-6 and GPR39 in skin fibroblasts by qPCR. As shown in Fig. 6C, the expression of IL-6 and GPR39 in the unwounded skin fibroblasts was very low. On the other hand, expression of IL-6 and GPR39 was increased in the wounded skin fibroblasts, suggesting that *gpr39*-expressed fibroblasts can produce IL-6 upon injury (Fig. 6C). Consistent with our observations, *Gpr39*^{-/-} mice showed impaired wound healing at the early stage in normal skin (Fig. 6D).

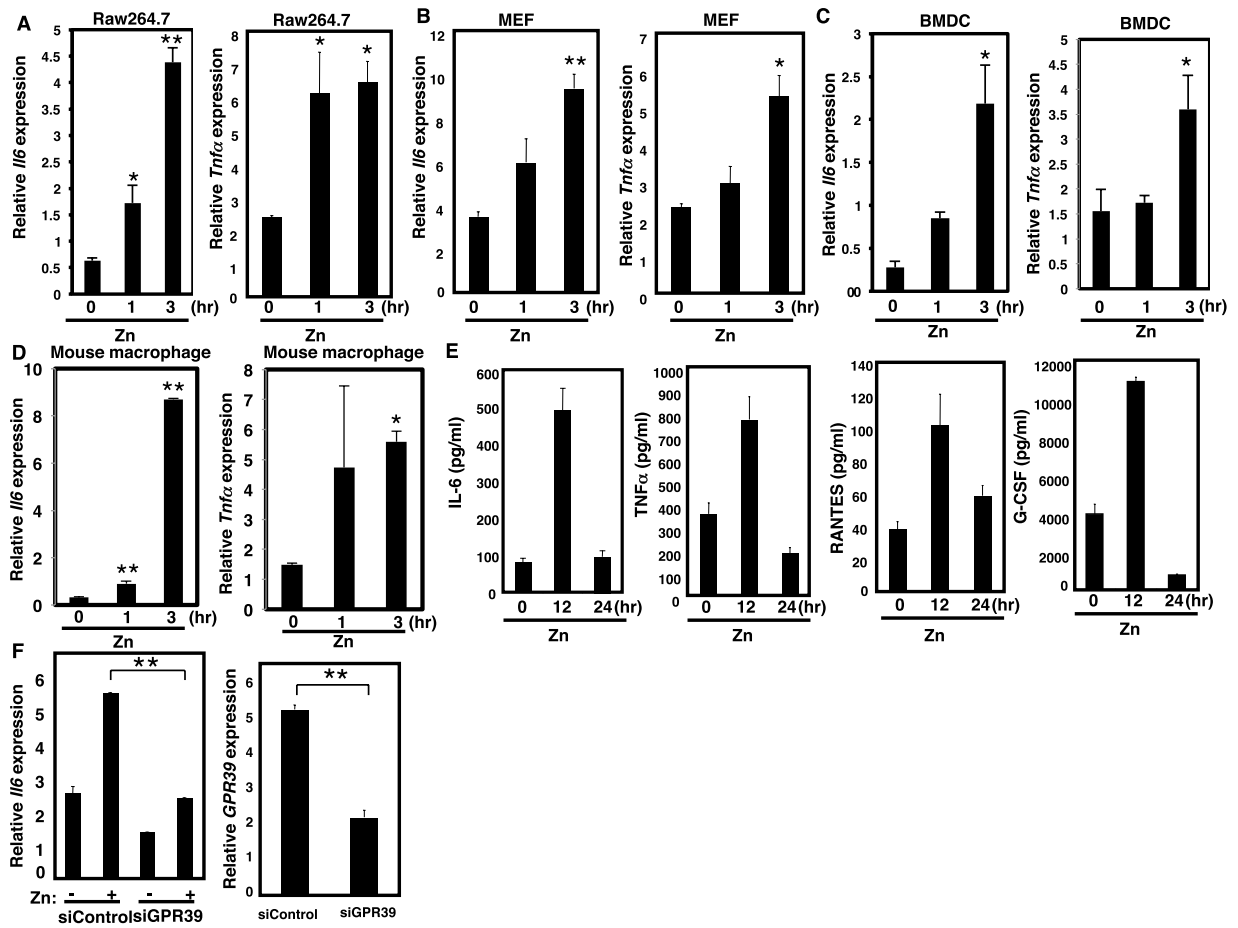


Figure 4. Zn can induce cytokine gene expression through GPR39. Zn-induced *Il-6* and *Tnfα* gene expression in (A) Raw264.7 cells, (B) MEFs, (C) BMDCs and (D) mouse macrophage. Values represent the mean + SD. (E) Zn-induced the expression of IL-6, TNFα, RANTES, and G-CSF protein in Raw264.7 cells, measured by the Bio-Plex suspension array system. (F) MEFs were transfected with siGPR39- or si-non-targeting control constructs, and cytokine or *Gpr39* gene expression was measured by real-time PCR. * $P < 0.05$, ** $P < 0.01$ (Tukey-Kramer multiple comparison test or two-tailed Student's t-test. A representative dataset from two (for d, e) or three (for a, b, c, f) experiments, each of which gave similar results, is shown.

Finally, we evaluated whether Zn injection into *Kit^{w-sh/w-sh}*, *ZnT2^{-/-}*, *GPR39^{-/-}*, and *IL-6^{-/-}* mice can restore wound healing deficiency in these mutant mice. As shown in Fig. 7A,B, addition of Zn to the wound area improved the delay in wound healing in *Kit^{w-sh/w-sh}* and *ZnT2^{-/-}* mice compared to their respective untreated controls. However, addition of Zn to the wound area in *GPR39^{-/-}* mice did not rescue the delay in wound healing in *GPR39^{-/-}* mice (Fig. 7C). Furthermore, addition of Zn to the wound area of *IL-6^{-/-}* mice rescued the delay in wound healing in *IL-6^{-/-}* mice compared to control mice, as shown in Fig. 7D. These results indicated that Zn directly promotes wound repair through Zn receptor GPR39.

Collectively, our findings indicated that Zn and mast cells regulate wound healing through GPR39-mediated IL-6 production by fibroblasts and perhaps other cell types. (Supplemental Fig. 14).

Discussion

It has long been known that Zn deficiency is associated with poor wound healing^{10,11}. This has largely been speculated to be due to the general role of Zn in DNA and protein synthesis⁴⁷. Thus, Zn is known to play an important role in promoting cutaneous wound healing, but its precise mechanism has not been fully understood. In this study, we used a combination of approaches including genetically engineered knockout mice, siRNA gene silencing, and signaling pathway inhibitors to investigate the role of Zn in wound healing and elucidate the mechanism by which it functions. Our findings demonstrate the following: (1) ZnT2 is required for the accumulation and release of Zn from mast cells, (2) Zn activates various types of cells and transmits intracellular signals through GPR39, (3) Zn/GPR39-mediated signaling induces the production of cytokines including the major inflammatory cytokine IL-6⁴⁸ via the PKC/MAPK/C/EBP pathway, and (4) ZnT2, IL-6, and GPR39 are all required in the early stage of normal wound healing. (5) Zinc supplementation can improve the delay in wound healing in mast cell-deficient *Kit^{w-sh/w-sh}* mice and zinc transporter-deficient *ZnT2^{-/-}* mice. Thus, our findings revealed a novel role of Zn and mast cells in inflammation. Our results clearly showed that Zn and mast cells are required for

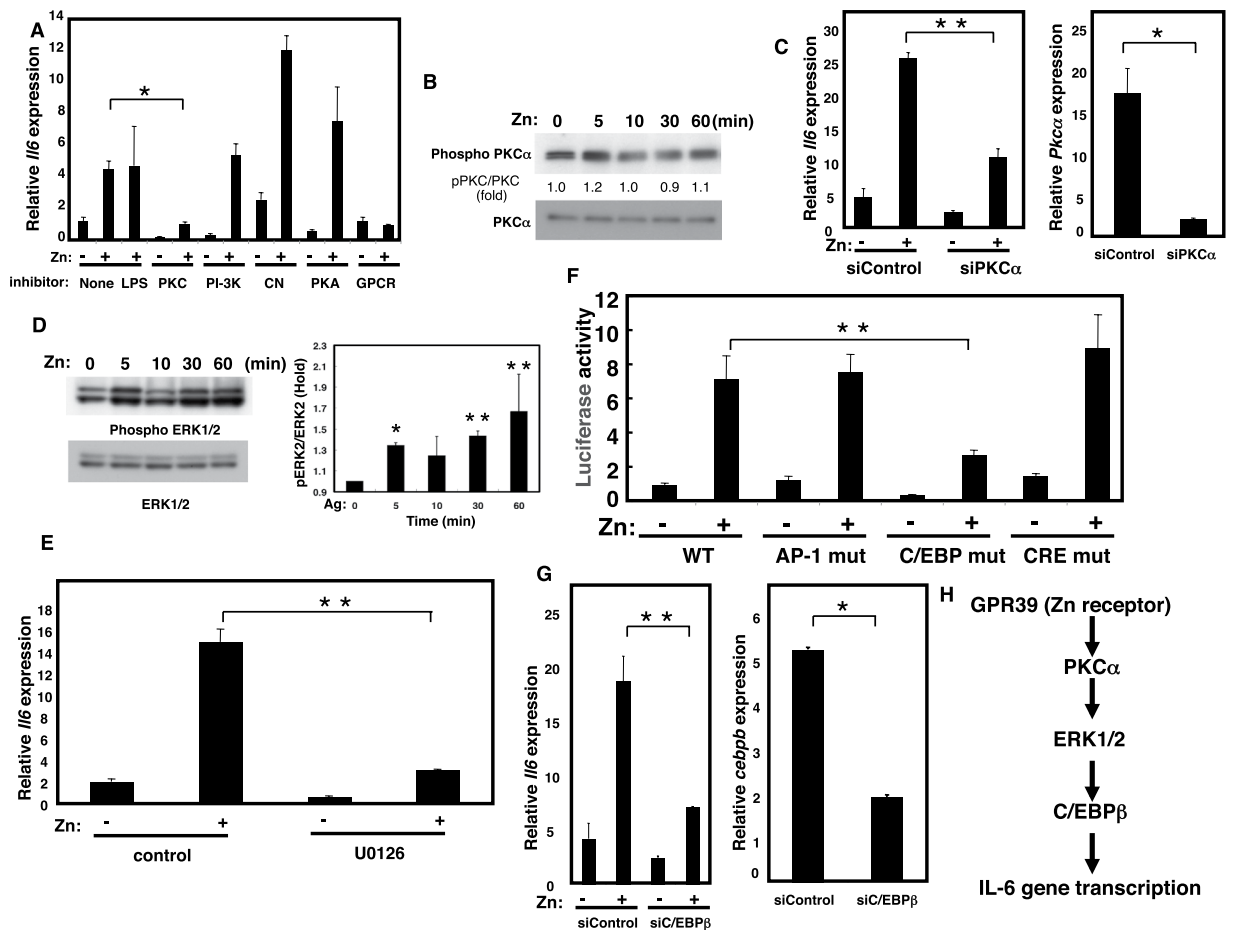


Figure 5. The PKC/MAPK/C/EBP-mediated signaling pathway regulates *Il-6* gene induction. (A) Raw264.7 cells were treated with 50 μ M Zn or 1 μ g/ml LPS. Zn-induced *Il-6* gene expression with PKC inhibitor Gö6976 (10 μ M), PI3K inhibitor wortmannin (500 nM), calcineurin inhibitor CsA (2.5 μ g/ml), PKA inhibitor 14–22 (1 μ M), or GPCR inhibitor GDP β S (1 mM). *Il-6* gene induction after Zn stimulation for 3 h was measured by real-time PCR. (B) Raw264.7 cells were treated with 50 μ M Zn, then PKC α phosphorylation was monitored. Quantification of PKC α phosphorylation normalized to the total PKC α level is shown in the middle. (C) MEFs were transfected with siPKC α – or si-non-targeting constructs, and the *Il-6* or *Pkc α* gene expression was measured by real-time PCR. (D) Raw264.7 cells were treated with 50 μ M Zn, then ERK1/2 phosphorylation was monitored. Quantification of ERK2 phosphorylation normalized to the total ERK2 level is shown in the right. * $P < 0.05$, ** $P < 0.01$ (two-tailed Student's *t*-test). (E) Raw264.7 cells were treated with 50 μ M Zn. Zn-induced *Il-6* gene induction with MEK inhibitor U0126 (50 μ M). *Il-6* induction after 3 h of Zn stimulation measured by real-time PCR. (F) Raw264.7 cells were stimulated with Zn, then tested for IL-6 reporter activity using the pGL4.21/human *Il-6* promoter (–1178/+13) and its mutant constructs (Supplemental Fig. 12). (G) MEFs were transfected with siCebpb- or si-non-targeting constructs, and *Il-6* or *Cebpb* gene expression was measured by real-time PCR. (H) A model for Zn-mediated cytokine gene induction. Zn binds to the Zn receptor GPR39, activating PKC which phosphorylates and activates ERK1/2. Phosphorylated ERK1/2 activates C/EBP β , which controls the *Il-6* gene expression. A representative dataset from two (for b) or three (for a, c, d, f, e, g) experiments, each of which gave similar results, is shown.

production of IL-6 via GPR39 in several different types of cells present at sites of inflammation, and we conclude that mast cells promote wound healing through the Zn/GPR39/IL-6 axis.

We and others have previously shown that IL-6 is required for normal wound healing^{49,50}. The wound healing process includes inflammation. During the inflammatory phase, platelet aggregation is followed by infiltration of leukocytes into the wound site. Cell debris and bacteria are phagocytosed and removed from the wound site by white blood cells. The inflammatory phase then transitions to the proliferative phase. We showed that the expression of *Il-6* mRNA was significantly reduced in the wounded *ZnT2*^{–/–} mice compared to wounded controls, suggesting IL-6 contributes to the inflammatory phase of wound healing. In addition, our results indicated that Zn receptor GPR39 on skin fibroblasts that receive Zn from mast cells spread IL-6 around the wound site. This idea is supported by the results showing defects in wound healing in *ZnT2*^{–/–}, *GPR39*^{–/–}, and *IL-6*^{–/–} mice. Indeed, it has been reported that GPR39 is involved in skin wound healing⁵¹. These results suggest that ZnT2-dependent GPR39/IL-6 axis can amplify the cytokine in the inflammatory phase of normal wound healing.

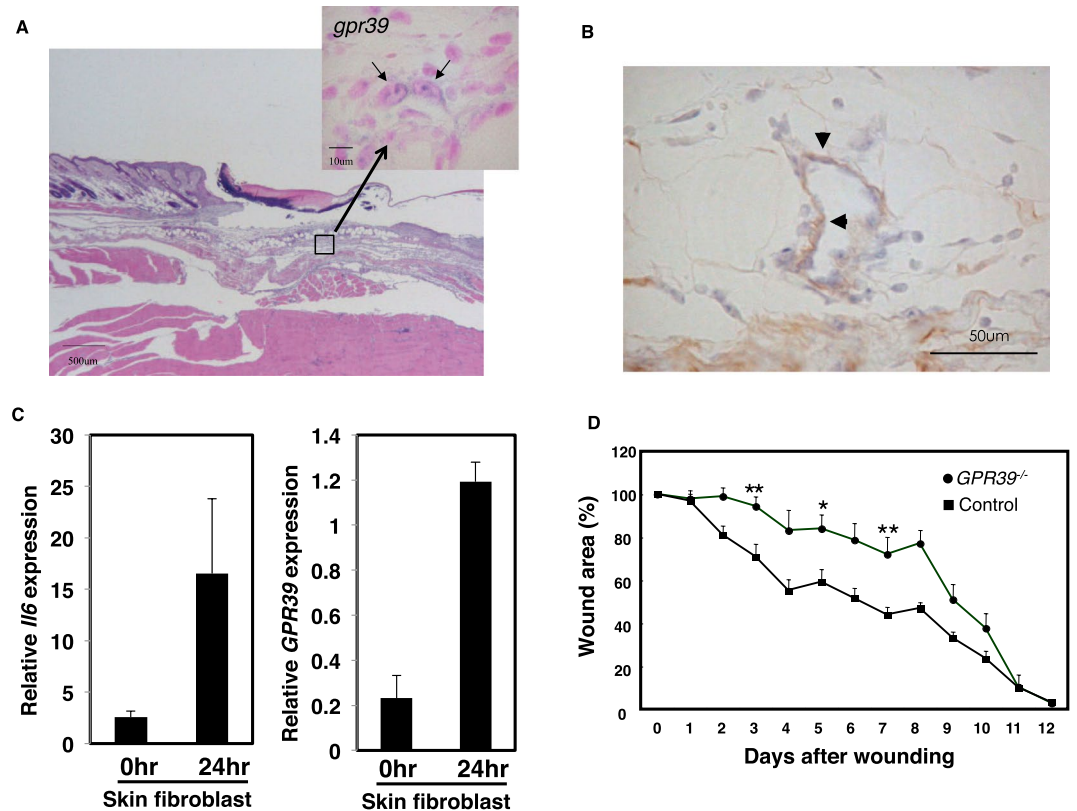


Figure 6. GPR39 is important for normal wound healing. (A) *In situ* hybridization analysis of skin wound samples from WT mice 3 days after injury. Skin samples were hybridized with a *Gpr39*-specific probe. Enlarged image of the boxed area is shown (upper right). The bar indicates 10 μ m. (B) *In situ* hybridization and immunohistochemistry analysis of skin wound samples from WT mice 3 days after injury. Skin samples were hybridized with a *Gpr39*-specific probe. Skin fibroblast was then detected with anti-fibroblasts antibody (clone ER-TR7). The arrowhead indicates *Gpr39* and fibroblast double-positive cell in the skin. The bar indicates 50 μ m. (C) Real time-PCR analysis of skin fibroblast samples from WT mice 1 days after injury. The expression of *Il-6* (left panel) and *Gpr39* (right panel) were examined by real time-PCR analysis. Relative expressions were normalized against *G3pdh*. Data are means \pm SD (n = 4 to 6). (D) Wound repair was evaluated in *Gpr39*^{-/-} and control mice as in Fig. 2A. Values represent the mean \pm SEM. Filled circles, *Gpr39*^{-/-} (n = 8 animals; female = 5, male = 3); filled squares, control (n = 10 animals; female = 6, male = 4). *P < 0.05, **P < 0.01 (two-tailed Student's t-test), *Gpr39*^{-/-} compared with control mice.

Zn was previously reported as a potential endogenous agonist for GPR39, but the physiological ligand for this receptor has not been identified^{45,46}. Our results demonstrate that Zn is indeed a physiological ligand and an agonist for GPR39 at sites of inflammation. Furthermore, we presented evidence that directly link extracellular Zn to intracellular signaling and cytokine production. We showed that Zn can activate the PKC/MAPK/C/EBP signaling cascade leading to *Il-6* gene induction. We showed that the G-protein inhibitor GDP β S blocked the effect of Zn on cytokine gene expression, indicating that the Zn receptor GPR39 utilizes G protein to transmit downstream target molecules. Previous reports showing that the activation of GPR39 by Zn stimulates both PLC activity and cAMP production through G α supports this result^{31,46}. It is well known that PLC hydrolyzes phosphatidylinositol 4,5-bisphosphate (PIP₂) to diacylglycerol (DAG) and inositol triphosphate (IP₃) and that DAG activates PKC. Furthermore, ERK can phosphorylate C/EBP, promoting its nuclear translocation⁵². These reports combined with our observations strongly suggest that the GPR39/PKC/MAPK/C/EBP signaling cascade is required for Zn-mediated cytokine gene induction and this mechanism may share a common role in Zn-dependent inflammatory disorders.

Our studies also revealed the role of ZnT2 in the accumulation of Zn in mast cell granules. Similarly, ZnT3 was shown to be required for the accumulation of Zn in neuronal synaptic vesicles prior to its release as a neurotransmitter^{38,53}. The ZnT2 expression is primarily confined to specialized secretory tissues such as the mammary and prostate glands⁵⁴. Recent studies that identified a genetic mutation in *ZnT2* in women producing breast milk with low concentration of Zn that causes severe neonatal Zn deficiency suggested that ZnT2 is essential for the optimal secretion of Zn into milk from the mammary gland⁵⁵. In addition, ZnT8 is required for the accumulation of Zn in the insulin granules in pancreatic β -cells where Zn regulates insulin clearance⁵⁶. Collectively, these reports and the results of our current study demonstrate the critical role of the ZnT family in the accumulation of Zn in cellular organelles as well as the physiological roles of released Zn.

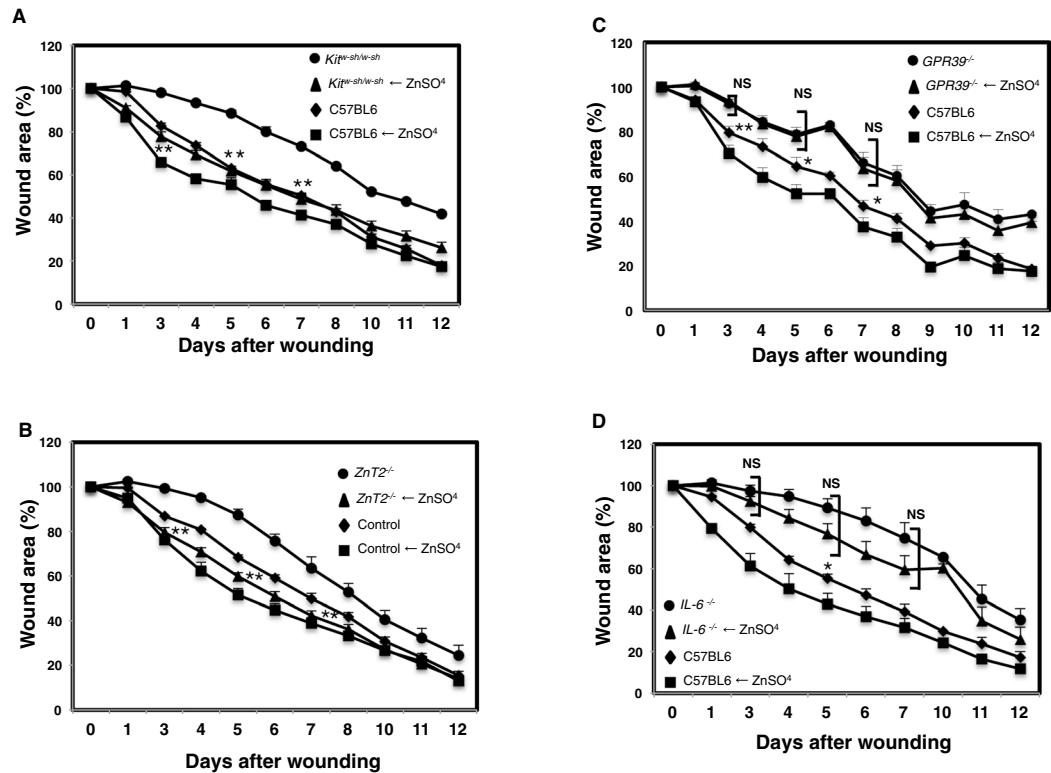


Figure 7. Zn is required for normal wound healing. Wound repair was evaluated in Zn-treated *Kit^{W-sh}/Kit^{W-sh}*, *ZnT2^{-/-}*, *Gpr39^{-/-}*, *Il-6^{-/-}*, and control mice. Values represent the mean + SEM. (A) Wound repair monitored over 12 days in Zn treated-*Kit^{W-sh}/Kit^{W-sh}* mice and control mice. Changes in the wound area in *Kit^{W-sh}/Kit^{W-sh}* (n = 6 animals; female = 2, male = 4, filled circles), Zn-treated *Kit^{W-sh}/Kit^{W-sh}* (n = 6, animals; female = 2, male = 4, filled triangles), control (n = 5, animals; female = 3, male = 2, filled diamonds), Zn-treated control (n = 5, animals; female = 2, male = 3, filled squares). **P < 0.01 (two-tailed Student's t-test), *Kit^{W-sh}/Kit^{W-sh}* compared with Zn-treated *Kit^{W-sh}/Kit^{W-sh}* mice. (B) Wound repair monitored over 12 days in Zn-treated *ZnT2^{-/-}* mice and control mice. Changes in the wound area in *ZnT2^{-/-}* mice (n = 6, animals; female = 2, male = 4, filled circles), Zn-treated *ZnT2^{-/-}* mice (n = 6, animals; female = 3, male = 3, filled triangles), control (n = 5, animals; female = 2, male = 3, filled diamonds), Zn-treated control (n = 6, animals; female = 2, male = 4, filled squares). **P < 0.01 (two-tailed Student's t-test), *ZnT2^{-/-}* compared with Zn-treated *ZnT2^{-/-}* mice. (C) Wound repair monitored over 12 days in Zn treated- *Gpr39^{-/-}* mice and control mice. Changes in the wound area in *Gpr39^{-/-}* (n = 7, animals; female = 5, male = 2, filled circles), Zn-treated *Gpr39^{-/-}* (n = 7, animals; female = 3, male = 4, filled triangles), control (n = 5, animals; female = 2, male = 3, filled diamonds), Zn-treated control (n = 6, animals; female = 3, male = 2, filled squares). N.S., not significant, *P < 0.05, **P < 0.01 (two-tailed Student's t-test), Statistical significance between Zn-treated *Gpr39^{-/-}* and control mice is shown. (D) Wound repair monitored over 12 days in Zn treated- *Il-6^{-/-}* mice and control mice. Changes in the wound area in *Il-6^{-/-}* (n = 5, animals; female = 2, male = 3, filled circles), Zn-treated *Il-6^{-/-}* (n = 6, animals; female = 4, male = 2, filled triangles), control (n = 4, animals; female = 1, male = 3, filled diamonds), Zn-treated control (n = 4, animals; female = 1, male = 3, filled squares). Statistical significance between Zn-treated *Il-6^{-/-}* and control mice is shown. N.S., not significant, *P < 0.05.

Our findings provide new insights into the molecular mechanisms of wound healing involving mast cells. Our data showing that IL-6 is a major inflammatory cytokine with key roles in autoimmune and inflammatory diseases suggest that the Zn/GPR39/IL-6/cytokine axis may be involved in a variety of inflammatory diseases^{48,57}. In addition, many cells have Zn-containing granules and are likely to release it upon stimulation^{25,26,58–60}, and cells in inflammatory tissues such as fibroblasts, macrophages, and dendritic cells, express GPR39 as shown in our data. This study paves the way for future research on therapeutic targets in inflammatory diseases for which Zn-containing cells and other inflammatory cells that affect the Zn/GPR39/IL-6/signaling axis are responsible.

Methods

Mice. C57BL/6J mice were obtained from CREA Japan. Mast cell-deficient *Kit^{W-sh}/Kit^{W-sh}* mice were provided by the RIKEN BioResource Center (RBRC No. RBRC01888) and have been backcrossed at least 10 times to C57BL/6 at RIKEN. *Il-6^{-/-}* mice (kindly provided by M. Kopf, Max-Planck-Institute of Immunobiology, Germany, and Y. Iwakura, Tokyo University of Science, Japan) were backcrossed with C57BL/6 mice for >10 generations. *Gpr39^{-/-}* mice were generated by Deltagen (San Mateo, CA, USA)⁶¹ and backcrossed to a C57BL/6 background for 5 generations. Mast-TRECK mice were provided by Dr. M. Kubo (kindly provided by Tokyo University of Science, Japan). Mas-TRECK tg mice received intraperitoneal injection of 250 ng diphtheria toxin (D0564, Sigma)

for 5 consecutive days⁶². Mice used for all experiments were between 6–11 weeks of age. We obtained approval from the Animal Research Committee at RIKEN and the animal research committee at Suzuka University of Medical Science for all animal experiments performed in this study. All methods were performed in accordance with the relevant guidelines and regulations.

Antibodies and reagents. Anti-ZnT2 antibodies were raised by immunizing rabbits with KLH-conjugated peptide (GKFNHHTMTIQIEKYSSEDMKNCQACQGPLE). The rabbits were first injected with 200 µg of KLH-conjugated ZnT2 peptide in complete Freund's adjuvant and then boosted every week with 50 µg of the antigen in incomplete Freund's adjuvant. Anti-CD63 (D263-3) antibody was purchased from MBL. Anti-PKCα (SC-208, C-20), anti-phospho-PKC (9371S, S660), anti-GPR39 (ab39227), anti-phospho ERK1/2 (V803A), and anti-ERK1/2 (V114A) antibodies were obtained from Santa Cruz, Cell Signaling, Abcam, and Promega, respectively. Gö6976 (365250), Wortmannin (681675), Cyclosporin A (239835), PKA inhibitor 14–22 (476485), GDPβS (371543), and U0126 (662005) were purchased from Calbiochem. LPS (L2637, LPS from *Escherichia coli* O55:B5) was purchased from SIGMA.

Cell lysates and immunoblotting. Cells were harvested, lysed with lysis buffer (20 mM Tris-HCl pH 7.4, 150 mM NaCl, 1% NP-40, proteinase inhibitors, 5 µg/ml pepstatin, 10 µg/ml leupeptin) for 30 min at 4 °C and spun at 12,000 × g, 4 °C for 30 min. The eluted and reduced samples were resolved by SDS-PAGE using a 5–20% gradient polyacrylamide gel (197–15011, Wako), and transferred to a PVDF membrane (IPVH00010, Immobilon-P, Millipore). For immunoblotting, the membranes were incubated with primary antibodies. The membranes were then incubated with HRP-conjugated anti-mouse (62–6520, Thermo Fisher Scientific) or anti-rabbit (65–6120, Thermo Fisher Scientific) antibody for 1 h at room temperature. After extensive washing of the membranes, immunoreactive proteins were visualized using the Western Lightning-ECL system (RPN2232, GE-Healthcare), according to the manufacturer's instructions. The PVDF membranes were exposed to Fuji RX film (Fuji, RX-U) and densitometric analysis was performed using an LAS-1000 fluorescence image analyzer (Fujifilm, Japan)¹⁸.

Wounding and measurement of the wound area. Full-thickness wounds (one per mouse) were induced on the lower back skin of mice as described previously⁴³. Mice were used at 6–11 weeks of age, when all the hair follicles on the back skin were in the telogen (resting) phase of the hair cycle. Briefly, the dorsal hair was shaved 24 h before wounding. Mice were anesthetized intraperitoneally with Somnopentyl, and the skin was wiped with 70% ethanol and then wounded using a 6 mm-diameter biopsy punch (BP-60F, Kai Industries, Tokyo, Japan). The wound area was evaluated at various time points after wounding by measuring the diameters along the rostrocaudal and perpendicular (left-right) axes with an ABS Digimatic Caliper (Mitutoyo, Japan) and then calculating the area. The change in wound area was expressed as the percentage of the initial wound area.

Mast cell engraftment. Mast cell engraftment was prepared as described previously⁴³. BMMCs derived from *ZnT2*^{-/-} and *ZnT2*^{+/+} mice were transferred by intradermal injection (10⁶ in 200 µl DMEM per cm², 20 injections of 10 µl each) into an area of 4 cm² on the back skin of 4-week-old *Kit*^{W^{sh}/W^{sh} mice. Four weeks after adoptive transfer of BMMCs, mice were used for experiments. To observe the skin mast cells, paraffin sections were fixed and stained with nuclear fast red and Alcian blue or Toluidine blue, and the Alcian blue or Toluidine blue-stained cells in each sample were counted.}

Primary mast cell cultures and cell lines. BMMCs (bone-marrow derived mast cells), BMDCs (bone-marrow derived dendritic cells), and peritoneal macrophages were prepared as described^{18,63–65}. For the preparation of BMMCs, bone-marrow cells obtained from 8-week-old C57BL/6J or BALB/c mice were cultured in RPMI 1640 supplemented with 10% heat-inactivated FBS, 10 mU/mL penicillin, 0.1 mg/mL streptomycin and the culture supernatant of IL-3-producing CHO cells (CHOmIL-3-3-12M; a gift from T. Sudo, Toray Industry, Kanagawa, Japan), and incubated in a humidified 5% CO₂ and 95% air at 37 °C. After 4–5 weeks of culturing, cell-surface expression of FcεRI and c-Kit was confirmed and these cells were used for experiments (<95% mast cells). For the preparation of BMDCs, BMDCs were generated from bone marrow cells with RPMI 1640 medium containing 10% FCS in the presence of murine GM-CSF (20 ng/ml, PEPRO TECH, AF-315-03) or the culture supernatant of GM-CSF-producing CHO cells, as described previously⁶⁴. Loosely adherent clustering cells were harvested on days 6–8, and CD11c⁺ DCs were isolated by the IMag Cell Separation System with anti-CD11c mAb-bound beads or FACSAria (BD Biosciences). The sorted CD11c⁺ DCs were immature (CD11c^{high} MHC class II^{low}), and the purity was >95%. For the preparation of peritoneal macrophages, C57BL/6J mice received an intraperitoneal (i.p.) injection of 1 ml of 3% (w/v) thioglycollate. Four to five days after injection, the peritoneal macrophages were collected by flushing the peritoneal cavity and were cultured in RPMI medium containing 10% FBS. Raw264.7 cells and MEFs were maintained in RPMI1640 supplemented with 10% FBS, penicillin and streptomycin. MEFs were prepared from C57BL/6J fetuses (13.5 days postcoitus)⁶⁶.

RNA interference for GPR39, PKCα and C/EBPβ. To knock down GPR39, PKCα, and C/EBPβ, MEFs were transfected with small interfering RNA (siRNA) against GPR39, PKCα, and C/EBPβ or with nontargeting siRNA (SMARTpool; GE-Healthcare) using Lipofectamine RNAiMAX (13778-150, Thermo Fisher Scientific), according to the manufacturer's instructions. Briefly, MEFs (5 × 10⁵ cell per well) were transfected with siRNA to a final concentration of 200 nM using Lipofectamine RNAiMAX. Forty-eight hours later, cells were stimulated with 50 µM Zn for 3 hrs followed by real-time Quantitative RT-PCR analysis to determine changes in the level of transcription.

Measurement of cytokines. Raw264.7 cells (0.5×10^5 cells) were treated with $50 \mu\text{M}$ Zn for 12 and 24 hrs. Cytokines were analyzed by the Bio-Plex suspension array system (Bio-Rad) according to the manufacturer's protocol.

Measurement of Zn. Extracts from BMDCs (0.9×10^6 cells) were diluted with water to a total volume of 25 ml and maintained under acidic conditions with nitric acid. Concentrations of Zn^{2+} ions in the diluted extracts were measured by an ICP-AA spectrometer (Shimadzu Sequential Plasma Spectrometer ICPS-8100, Japan) calibrated using calibration curves in the range of 0 to 100 ppb of Zn^{2+} .

Confocal microscopy. BMDCs were allowed to adhere to glass slides (Matsunami, Japan). In some experiments, $10 \mu\text{M}$ FluoZin-3 (F-24195, Thermo Fisher Scientific) was added for 30 min, and the cells were then fixed with 4% paraformaldehyde in PBS. BMDCs were immunostained after being permeabilized with BD Perm/Wash buffer (554723, BD Biosciences). Antibodies were diluted in buffer containing 1% BSA (anti-ZnT2 at a dilution of 1:25 and anti-CD63 at 1:100). The cells were washed with PBS, then mounted with Mounting Medium (S302380, Dako Cytomation). Confocal microscopy was carried out using the TCS SL system (Leica, Germany). Images were transferred to Adobe Photoshop CS3.

Electron microscopy. Electron microscopic observation was carried out by the silver-intensified immunogold method. Cryostat sections from the cell pellets were incubated with anti-CD63 or anti-ZnT2 antibodies, followed by an incubation with goat anti-rat IgG or anti-rabbit IgG covalently linked 1-nm gold particles (1:200; Nanoprobes, Yaphank, NY). After silver enhancement using a kit (HQ silver; Nanoprobes), the sections were osmicated, dehydrated, and directly embedded in Epon (Nissin EM, Tokyo, Japan). Ultrathin sections were prepared and stained with both uranyl acetate and lead citrate for observation under an electron microscope (H-7100; Hitachi, Tokyo, Japan).

Histological and *in situ* hybridization analyses. Mouse tissue, fixed with G-Fix (Genostaff), was embedded in paraffin on CT-Pro20 (Genostaff) using G-Nox (Genostaff) as a less toxic organic solvent for xylene, and sectioned at $4 \mu\text{m}$.

In situ hybridization was performed using the ISH Reagent Kit (Genostaff) according to the manufacturer's instructions. Tissue sections were deparaffinized with G-Nox, and rehydrated through a graded series of ethanol and PBS. The sections were fixed with 10% NBF (10% Formalin in PBS) for 30 min at 37°C and washed in distilled water, placed in 0.2% HCl for 10 min at 37°C and washed in PBS, treated with $15 \mu\text{g}/\text{ml}$ Proteinase K (Wako Pure Chemical Industries) in PBS for 10 min at 37°C and washed in PBS, then placed within a coplin jar containing 1xG-Wash (Genostaff), equal to 1xSSC. Hybridization was performed with probes for *Gpr39* at concentrations of $250 \text{ ng}/\text{ml}$ in G-Hybo-L (Genostaff) for 16 hr at 60°C . After hybridization, the sections were washed in 1xG-Wash for 10 min at 60°C , 50% formamide in 1xG-Wash for 10 min at 60°C . Then the sections were washed twice in 1xG-Wash for 10 min at 60°C twice in 0.1xG-Wash for 10 min at 60°C , and twice in TBST (0.1% Tween20 in TBS) at RT. After treatment with 1xG-Block (Genostaff) for 15 min at RT, the sections were incubated with anti-DIG AP conjugate (Roche Diagnostics) diluted 1:2000 with x50G-Block (Genostaff) in TBST for 1 hr at RT. The sections were washed twice in TBST and then incubated in 100 mM NaCl, 50 mM MgCl_2 , 0.1% Tween20, 100 mM Tris-HCl, pH 9.5. Color development was performed with NBT/BCIP solution (Sigma-Aldrich) overnight, then samples were washed using PBS⁶⁷.

For IHC as a second staining after ISH, endogenous peroxidase was blocked with 0.3% H_2O_2 in PBS for 30 min, then sections were incubated with G-Block (Genostaff) and Avidin/Biotin Blocking Kit (Vector Laboratories). The sections were incubated with $2 \mu\text{g}/\text{mL}$ of anti-Fibroblasts rat monoclonal antibody (ER-TR7, LifeSpan BioSciences) at $2-8^\circ\text{C}$ overnight. They were incubated with biotin-conjugated rabbit anti-rat IgG (Vector), for 30 min at RT, followed by the addition of peroxidase conjugated streptavidin (Nichirei) for 5 min. Peroxidase activity was visualized by diaminobenzidine and then washed with tap-water. Then, the sections were mounted with G-Mount (Genostaff).

Skin fibroblast isolation. In order to obtain murine skin cells, skin was collected from the back and cut into small pieces and treated with 0.1% collagenase (Wako, 032-22364) as described previously⁶⁸. Following the collagenase treatment, cells were filtered through $70 \mu\text{m}$ cell strainer (BD Biosciences, 352350) and washed with 2% NCS (Gibco, 15070063) containing RPMI1640 (nacalai tesque, 30264-56) medium. Cell sorting was conducted with FACS Aria III. Collected cells were first stained with Fc-block (BD Biosciences, 553141). Cells were then washed and stained with anti-mouse antibodies and 7-AAD. The staining patterns used for skin fibroblasts were $\text{CD90.2}^+ \text{gp38}^+ \text{CD45}^{\text{neg}}$.

Real-time quantitative RT-PCR analysis. Cells were homogenized with Sepasol RNAI (nacalai tesque, 09379-55), and the total RNA was isolated following the manufacturer's instructions. For standard RT-PCR, cDNA was synthesized from 500 ng of total RNA with reverse transcriptase (TRT-101, ReverTra Ace; Toyobo) and 500 ng of oligo (dT) primer (Invitrogen) for 30 min at 42°C . A portion of the cDNA (typically 1/20 volume) was used for standard PCR to detect *Il-6*, *Tnf α* , *Tgf β 1* and *G3pdh*. Twenty-five cycles of PCR were performed with 0.5 U of rTaq DNA polymerase and 10 pmol of gene-specific sense and antisense primers. For real-time quantitative RT-PCR, the *Il-6* or *Tnf α* gene expression was measured relative to *G3pdh* using the SYBR[®] Green reagent (RR820A, TaKaRa)^{18,69}. The primers used in these experiments were purchased from TaKaRa, and the sequences are as follows: *Il-6*: forward primer, 5'-GAGGATACCACTCCCAACAGACC-3' and reverse primer, 5'-AAGTGCATCATCGTTGTTCATACA-3'; *TNF α* : forward primer, 5'-CATCTTCTCAAATTCGAGTGACAA-3' and reverse primer, 5'-TGGGAGTAGACAAGGTACAA CCC-3'; *TGF β 1*: forward primer, 5'-GTGTGGAGCAACATGTGGAACCTTA-3' and reverse primer, 5'-CGCTGAA TCGAAAGCCCTGTA-3'. *G3PDH*: forward primer, 5'-TTCACCACCATGGAGAAGGCCG-3' and reverse primer, 5'-GGCATGGACTGTGGTCATGA-3'.

Luciferase reporter assay. The pGL4.21/human *IL-6* promoter (−1178/+13) vector and pRL-TK vector were transiently cotransfected into Raw264.7 cells using the Lipofectamine 2000 transfection reagent (11668019, Thermo Fisher Scientific). Cells were harvested 24 h after transfection and stimulated with the indicated reagents for 5 h. The Luciferase activity of the total cell lysates was measured using the Dual-Luciferase Reporter Assay System (E1910, Promega).

Statistical analysis. All data were analyzed with Statcel. Data were considered statistically significant when the *P* value was less than 0.05. Statistical analyses were performed using two-tailed Student's *t*-test. Additional statistical analyses were performed using Tukey-Kramer multiple comparison test.

References

- Prasad, A. S. Discovery of human zinc deficiency: its impact on human health and disease. *Adv Nutr* **4**, 176–190, <https://doi.org/10.3945/an.112.003210> (2013).
- Takahashi, H. *et al.* Effects of zinc deficient diet on development of atopic dermatitis-like eruptions in DS-Nh mice. *J Dermatol Sci* **50**, 31–39, <https://doi.org/10.1016/j.jdermsci.2007.11.002> (2008).
- Keen, C. L. & Gershwin, M. E. Zinc deficiency and immune function. *Annu Rev Nutr* **10**, 415–431, <https://doi.org/10.1146/annurev.nu.10.070190.002215> (1990).
- Ogawa, Y., Kawamura, T. & Shimada, S. Zinc and skin biology. *Arch Biochem Biophys* **611**, 113–119, <https://doi.org/10.1016/j.abb.2016.06.003> (2016).
- Hirano, T. *et al.* Roles of zinc and zinc signaling in immunity: zinc as an intracellular signaling molecule. *Adv Immunol* **97**, 149–176, [https://doi.org/10.1016/S0065-2776\(08\)00003-5](https://doi.org/10.1016/S0065-2776(08)00003-5) (2008).
- Nishida, K., Fukada, T., Yamasaki, S., Murakami, M. & Hirano, T. *Zinc in allergy, autoimmune, and hard and connective tissue diseases.* (IOS Press, 2011).
- Fukada, T., Yamasaki, S., Nishida, K., Murakami, M. & Hirano, T. Zinc homeostasis and signaling in health and diseases: Zinc signaling. *J Biol Inorg Chem* **16**, 1123–1134, <https://doi.org/10.1007/s00775-011-0797-4> (2011).
- Wessels, I., Maywald, M. & Rink, L. Zinc as a Gatekeeper of Immune Function. *Nutrients* **9**, <https://doi.org/10.3390/nu9121286> (2017).
- Lin, P. H. *et al.* Zinc in Wound Healing Modulation. *Nutrients* **10**, <https://doi.org/10.3390/nu10010016> (2017).
- Pories, W. J., Henzel, J. H., Rob, C. G. & Strain, W. H. Acceleration of wound healing in man with zinc sulphate given by mouth. *Lancet* **1**, 121–124 (1967).
- Pories, W. J., Henzel, J. H., Rob, C. G. & Strain, W. H. Acceleration of healing with zinc sulfate. *Ann Surg* **165**, 432–436 (1967).
- Andreini, C., Banci, L., Bertini, I. & Rosato, A. Counting the zinc-proteins encoded in the human genome. *J Proteome Res* **5**, 196–201, <https://doi.org/10.1021/pr050361j> (2006).
- Yamasaki, S. *et al.* Zinc is a novel intracellular second messenger. *J Cell Biol* **177**, 637–645, <https://doi.org/10.1083/jcb.200702081> (2007).
- Haase, H. & Rink, L. Functional significance of zinc-related signaling pathways in immune cells. *Annu Rev Nutr* **29**, 133–152, <https://doi.org/10.1146/annurev-nutr-080508-141119> (2009).
- Taylor, K. M., Kille, P. & Hogstrand, C. Protein kinase CK2 opens the gate for zinc signaling. *Cell Cycle* **11**, 1863–1864, <https://doi.org/10.4161/cc.20414> (2012).
- Nishida, K. & Yamasaki, S. In Zinc Signals in Cellular Functions and Disorders. *Springer*, 89–109 (2014).
- Nishida, K. & Uchida, R. Regulatory Mechanism of Mast Cell Activation by Zinc Signaling. *Yakugaku Zasshi* **137**, 495–501, <https://doi.org/10.1248/yakushi.16-00239-1> (2017).
- Uchida, R., Xiang, H., Arai, H., Kitamura, H. & Nishida, K. L-type calcium channel-mediated Zinc wave is involved in the regulation of IL-6 by stimulating non-IgE with LPS and IL-33 in mast cells and dendritic cells. *Biol Pharm Bull*, <https://doi.org/10.1248/bpb.b18-00565> (2018).
- Yamasaki, S. *et al.* A novel role of the L-type calcium channel $\alpha 1D$ subunit as a gatekeeper for intracellular zinc signaling: zinc wave. *PLoS One* **7**, e39654, <https://doi.org/10.1371/journal.pone.0039654> (2012).
- Frederickson, C. Imaging zinc: old and new tools. *Sci STKE* **2003**, pe18, <https://doi.org/10.1126/stke.2003.182.pe18> (2003).
- Frederickson, C. J., Koh, J. Y. & Bush, A. I. The neurobiology of zinc in health and disease. *Nat Rev Neurosci* **6**, 449–462, <https://doi.org/10.1038/nrn1671> (2005).
- Li, Y., Hough, C. J., Frederickson, C. J. & Sarvey, J. M. Induction of mossy fiber- \rightarrow Ca $_3$ long-term potentiation requires translocation of synaptically released Zn $^{2+}$. *J Neurosci* **21**, 8015–8025 (2001).
- Brown, C. E. & Dyck, R. H. Rapid, experience-dependent changes in levels of synaptic zinc in primary somatosensory cortex of the adult mouse. *J Neurosci* **22**, 2617–2625, doi:20026255 (2002).
- Howell, G. A., Welch, M. G. & Frederickson, C. J. Stimulation-induced uptake and release of zinc in hippocampal slices. *Nature* **308**, 736–738 (1984).
- Gustafson, G. T. Heavy metals in rat mast cell granules. *Lab Invest* **17**, 588–598 (1967).
- Ho, L. H. *et al.* Labile zinc and zinc transporter ZnT4 in mast cell granules: role in regulation of caspase activation and NF- κ B translocation. *J Immunol* **172**, 7750–7760, <https://doi.org/10.4049/jimmunol.172.12.7750> (2004).
- Popovics, P. & Stewart, A. J. GPR39: a Zn(2+)-activated G protein-coupled receptor that regulates pancreatic, gastrointestinal and neuronal functions. *Cell Mol Life Sci* **68**, 85–95, <https://doi.org/10.1007/s00018-010-0517-1> (2011).
- Sharir, H., Zinger, A., Nevo, A., Sekler, I. & Hershinkel, M. Zinc released from injured cells is acting via the Zn $^{2+}$ -sensing receptor, ZnR, to trigger signaling leading to epithelial repair. *J Biol Chem* **285**, 26097–26106, <https://doi.org/10.1074/jbc.M110.107490> (2010).
- Moehars, D. *et al.* Altered gastrointestinal and metabolic function in the GPR39-obestatin receptor-knockout mouse. *Gastroenterology* **131**, 1131–1141, <https://doi.org/10.1053/j.gastro.2006.07.009> (2006).
- Mlyniec, K., Budziszewska, B., Reczynski, W., Sowa-Kucma, M. & Nowak, G. The role of the GPR39 receptor in zinc deficient-animal model of depression. *Behav Brain Res* **238**, 30–35, <https://doi.org/10.1016/j.bbr.2012.10.020> (2013).
- Hershinkel, M. The Zinc Sensing Receptor, ZnR/GPR39, in Health and Disease. *Int J Mol Sci* **19**, <https://doi.org/10.3390/ijms19020439> (2018).
- Lichten, L. A. & Cousins, R. J. Mammalian zinc transporters: nutritional and physiologic regulation. *Annu Rev Nutr* **29**, 153–176, <https://doi.org/10.1146/annurev-nutr-033009-083312> (2009).
- Jeong, J. & Eide, D. J. The SLC39 family of zinc transporters. *Mol Aspects Med* **34**, 612–619, <https://doi.org/10.1016/j.mam.2012.05.011> (2013).
- Dufner-Beattie, J., Langmade, S. J., Wang, F., Eide, D. & Andrews, G. K. Structure, function, and regulation of a subfamily of mouse zinc transporter genes. *J Biol Chem* **278**, 50142–50150, <https://doi.org/10.1074/jbc.M304163200> (2003).
- Hara, T. *et al.* Physiological roles of zinc transporters: molecular and genetic importance in zinc homeostasis. *J Physiol Sci* **67**, 283–301, <https://doi.org/10.1007/s12576-017-0521-4> (2017).

36. Kambe, T., Matsunaga, M. & Takeda, T. A. Understanding the Contribution of Zinc Transporters in the Function of the Early Secretory Pathway. *Int J Mol Sci* **18**, <https://doi.org/10.3390/ijms18102179> (2017).
37. McCormick, N. H., Hennigar, S. R., Kiselyov, K. & Kelleher, S. L. The biology of zinc transport in mammary epithelial cells: implications for mammary gland development, lactation, and involution. *J Mammary Gland Biol Neoplasia* **19**, 59–71, <https://doi.org/10.1007/s10911-013-9314-4> (2014).
38. Cole, T. B., Wenzel, H. J., Kafer, K. E., Schwartzkroin, P. A. & Palmiter, R. D. Elimination of zinc from synaptic vesicles in the intact mouse brain by disruption of the ZnT3 gene. *Proc Natl Acad Sci USA* **96**, 1716–1721 (1999).
39. Hijikata, A. *et al.* Construction of an open-access database that integrates cross-reference information from the transcriptome and proteome of immune cells. *Bioinformatics* **23**, 2934–2941, <https://doi.org/10.1093/bioinformatics/btm430> (2007).
40. Lee, S., Hennigar, S. R., Alam, S., Nishida, K. & Kelleher, S. L. Essential Role for Zinc Transporter 2 (ZnT2)-mediated Zinc Transport in Mammary Gland Development and Function during Lactation. *J Biol Chem* **290**, 13064–13078, <https://doi.org/10.1074/jbc.M115.637439> (2015).
41. Grose, R. & Werner, S. Wound-healing studies in transgenic and knockout mice. *Mol Biotechnol* **28**, 147–166, <https://doi.org/10.1385/MB:28:2:147> (2004).
42. Werner, S. & Grose, R. Regulation of wound healing by growth factors and cytokines. *Physiol Rev* **83**, 835–870, <https://doi.org/10.1152/physrev.00031.2002> (2003).
43. Weller, K., Foitzik, K., Paus, R., Syska, W. & Maurer, M. Mast cells are required for normal healing of skin wounds in mice. *FASEB J* **20**, 2366–2368, <https://doi.org/10.1096/fj.06-5837je> (2006).
44. Lai, Y. *et al.* Commensal bacteria regulate Toll-like receptor 3-dependent inflammation after skin injury. *Nat Med* **15**, 1377–1382, <https://doi.org/10.1038/nm.2062> (2009).
45. Yasuda, S. *et al.* Isolation of Zn²⁺ as an endogenous agonist of GPR39 from fetal bovine serum. *J Recept Signal Transduct Res* **27**, 235–246, <https://doi.org/10.1080/10799890701506147> (2007).
46. Holst, B. *et al.* GPR39 signaling is stimulated by zinc ions but not by obestatin. *Endocrinology* **148**, 13–20, <https://doi.org/10.1210/en.2006-0933> (2007).
47. Sandstead, H. H., Lanier, V. C. Jr., Shephard, G. H. & Gillespie, D. D. Zinc and wound healing. *Effects of zinc deficiency and zinc supplementation. Am J Clin Nutr* **23**, 514–519 (1970).
48. Hirano, T. Interleukin 6 in autoimmune and inflammatory diseases: a personal memoir. *Proc Jpn Acad Ser B Phys Biol Sci* **86**, 717–730, <https://doi.org/10.2183/pjab.86.717> (2010).
49. Gallucci, R. M. *et al.* Impaired cutaneous wound healing in interleukin-6-deficient and immunosuppressed mice. *FASEB J* **14**, 2525–2531, <https://doi.org/10.1096/fj.00-0073com> (2000).
50. Lin, Z. Q., Kondo, T., Ishida, Y., Takayasu, T. & Mukaida, N. Essential involvement of IL-6 in the skin wound-healing process as evidenced by delayed wound healing in IL-6-deficient mice. *J Leukoc Biol* **73**, 713–721 (2003).
51. Zhao, H. *et al.* GPR39 marks specific cells within the sebaceous gland and contributes to skin wound healing. *Sci Rep* **5**, 7913, <https://doi.org/10.1038/srep07913> (2015).
52. Lee, H. G. *et al.* Actin and ERK1/2-CEBPbeta signaling mediates phagocytosis-induced innate immune response of osteoprogenitor cells. *Biomaterials* **32**, 9197–9206, <https://doi.org/10.1016/j.biomaterials.2011.08.059> (2011).
53. Wenzel, H. J., Cole, T. B., Born, D. E., Schwartzkroin, P. A. & Palmiter, R. D. Ultrastructural localization of zinc transporter-3 (ZnT-3) to synaptic vesicle membranes within mossy fiber boutons in the hippocampus of mouse and monkey. *Proc Natl Acad Sci USA* **94**, 12676–12681 (1997).
54. Iguchi, K. *et al.* High-level expression of zinc transporter-2 in the rat lateral and dorsal prostate. *J Androl* **23**, 819–824 (2002).
55. Chowanadisai, W., Lonnerdal, B. & Kelleher, S. L. Identification of a mutation in SLC30A2 (ZnT-2) in women with low milk zinc concentration that results in transient neonatal zinc deficiency. *J Biol Chem* **281**, 39699–39707, <https://doi.org/10.1074/jbc.M605821200> (2006).
56. Tamaki, M. *et al.* The diabetes-susceptible gene SLC30A8/ZnT8 regulates hepatic insulin clearance. *J Clin Invest*, <https://doi.org/10.1172/JCI68807> (2013).
57. Murakami, M. *et al.* Disease-association analysis of an inflammation-related feedback loop. *Cell Rep* **3**, 946–959, <https://doi.org/10.1016/j.celrep.2013.01.028> (2013).
58. Emdin, S. O., Dodson, G. G., Cutfield, J. M. & Cutfield, S. M. Role of zinc in insulin biosynthesis. *Some possible zinc-insulin interactions in the pancreatic B-cell. Diabetologia* **19**, 174–182 (1980).
59. Giblin, L. J. *et al.* Zinc-secreting Paneth cells studied by ZP fluorescence. *J Histochem Cytochem* **54**, 311–316, <https://doi.org/10.1369/jhc.5A6724.2005> (2006).
60. Kelleher, S. L., McCormick, N. H., Velasquez, V. & Lopez, V. Zinc in specialized secretory tissues: roles in the pancreas, prostate, and mammary gland. *Adv Nutr* **2**, 101–111, <https://doi.org/10.3945/an.110.000232> (2011).
61. Holst, B. *et al.* G protein-coupled receptor 39 deficiency is associated with pancreatic islet dysfunction. *Endocrinology* **150**, 2577–2585, <https://doi.org/10.1210/en.2008-1250> (2009).
62. Sawaguchi, M. *et al.* Role of mast cells and basophils in IgE responses and in allergic airway hyperresponsiveness. *J Immunol* **188**, 1809–1818, <https://doi.org/10.4049/jimmunol.1101746> (2012).
63. Nishida, K. *et al.* Requirement of Gab2 for mast cell development and KitL/c-Kit signaling. *Blood* **99**, 1866–1869 (2002).
64. Kitamura, H. *et al.* Toll-like receptor-mediated regulation of zinc homeostasis influences dendritic cell function. *Nat Immunol* **7**, 971–977, <https://doi.org/10.1038/nl1373> (2006).
65. Wang, Q. *et al.* Anti-Inflammatory Profile of Levosimendan in Cecal Ligation-Induced Septic Mice and in Lipopolysaccharide-Stimulated Macrophages. *Crit Care Med* **43**, e508–520, <https://doi.org/10.1097/CCM.0000000000001269> (2015).
66. Itoh, M. *et al.* Role of Gab1 in heart, placenta, and skin development and growth factor- and cytokine-induced extracellular signal-regulated kinase mitogen-activated protein kinase activation. *Mol Cell Biol* **20**, 3695–3704 (2000).
67. Tsukasaki, M. *et al.* Host defense against oral microbiota by bone-damaging T cells. *Nat Commun* **9**, 701, <https://doi.org/10.1038/s41467-018-03147-6> (2018).
68. Kurashima, Y. *et al.* The enzyme Cyp26b1 mediates inhibition of mast cell activation by fibroblasts to maintain skin-barrier homeostasis. *Immunity* **40**, 530–541, <https://doi.org/10.1016/j.immuni.2014.01.014> (2014).
69. Kabu, K. *et al.* Zinc is required for Fc epsilon RI-mediated mast cell activation. *J Immunol* **177**, 1296–1305, <https://doi.org/10.4049/jimmunol.177.2.1296> (2006).

Acknowledgements

We thank Drs M. Kopf (Max-Planck-Institute of Immunobiology, Germany) and Y. Iwakura (Tokyo University of Science, Japan) for the IL-6-deficient mice. We thank Drs P. Burrows, M. Kato, and H. Kitamura for critical reading and Drs T. Tanaka, T. Kambe, T. Ugajin, S. Hida, and M. Hershinkel for technical advice and suggestions. We thank members of the RIKEN Center for Integrative Medical Sciences (IMS-RCAI) animal facility for helping to maintenance of various KO mice. This work was supported by Ms. C. Kariya, Materials Characterization Support Unit, Center for Emergent Matter Science RIKEN for the ICP-AES measurements. We thank A. Ito for excellent technical assistance and R. Kimura for secretarial assistance. This work was supported in part by

JSPS KAKENHI Grant Numbers JP16K15152 and JP18H05299 (K.N.), the Takeda Science Foundation (K.N.), the Mochida Memorial Foundation for Medical and Pharmaceutical Research (K.N.), and SENSHIN Medical Research Foundation (K.N.). This work was also supported by grants from Japan Agency for Medical Research and Development (H.K.); Japan Society for the Promotion of Science (JSPS), Grant-in Aid for Scientific Research S (H.K.) and Young Scientists A (Y.K.), Challenging Research or (Exploratory) (Y.K.), Leading Initiative for Excellent Young Researchers (LEADER) (Y.K.), Mochida Memorial Foundation for Medical and Pharmaceutical Research (Y.K.), The Takeda Science Foundation (Y.K.), The Uehara Memorial Foundation (Y.K.), GSK Japan Research Grant (Y.K.), Science and Technology Research Partnership for Sustainable Development (SATREPS) (H.K.) and the Chiba University-UC San Diego Center for Mucosal Immunology, Allergy, and Vaccines (H.K.). R.U. was supported by Nagai Memorial Research Scholarship from the Pharmaceutical Society of Japan, and Public Interest Incorporated Foundation Tsukushi Scholarship Research Fund.

Author Contributions

K.N., A.H., S.Y., R.U., W.O., Y.K., S.K., T.I. and H.O. performed the experiments; K.N., J.K., H.W., K.H., M.N., J.K., Y.O. and T.H. designed the research and analyzed the data; M.K., O.O., H.K., H.K. and M.M. play the manuscript with constructive discussions; K.N. and T.H. wrote the manuscript; and all authors reviewed and edited the manuscript.

Additional Information

Supplementary information accompanies this paper at <https://doi.org/10.1038/s41598-019-47132-5>.

Competing Interests: The authors declare no competing interests.

Publisher's note: Springer Nature remains neutral with regard to jurisdictional claims in published maps and institutional affiliations.



Open Access This article is licensed under a Creative Commons Attribution 4.0 International License, which permits use, sharing, adaptation, distribution and reproduction in any medium or format, as long as you give appropriate credit to the original author(s) and the source, provide a link to the Creative Commons license, and indicate if changes were made. The images or other third party material in this article are included in the article's Creative Commons license, unless indicated otherwise in a credit line to the material. If material is not included in the article's Creative Commons license and your intended use is not permitted by statutory regulation or exceeds the permitted use, you will need to obtain permission directly from the copyright holder. To view a copy of this license, visit <http://creativecommons.org/licenses/by/4.0/>.

© The Author(s) 2019